Sensitivity analysis of a flow redistribution model for a multidimensional and multifidelity simulation of fuel assembly bow in a pressurized water reactor

Ali Abboud, Stanislas de Lambert, Josselin Garnier, Bertrand Leturcq

SENSITIVITY ANALYSIS OF A FLOW REDISTRIBUTION MODEL FOR A MULTIDIMENSIONAL AND MULTIFIDELITY SIMULATION OF FUEL ASSEMBLY BOW IN A PRESSURIZED WATER REACTOR

Ali Abboud[1,2], Stanislas de Lambert[2], Josselin Garnier[1], Bertrand Leturcq[2]
[1] CMAP, CNRS, École polytechnique, Institut Polytechnique de Paris, 91120 Palaiseau, France
[2] Université Paris-Saclay, CEA, Service d'Études Mécaniques et Thermiques, 91191, Gif-sur-Yvette, France

email - ali.abboud@cea.fr

ABSTRACT

In the core of nuclear reactors, fluid-structure interaction and intense irradiation lead to progressive deformation of fuel assemblies. When this deformation is significant, it can lead to additional costs and longer fuel unloading and reloading operations. Therefore, it is preferable to adopt a fuel management that avoids excessive deformation and interactions between fuel assemblies. However, the prediction of deformation and interactions between fuel assemblies is uncertain. Uncertainties affect neutronics, thermohydraulics and thermomechanics parameters. Indeed, the initial uncertainties are propagated over several successive power cycles of twelve months each through the coupling of non-linear, nested and multidimensional thermal-hydraulic and thermomechanical simulations. In this article, we set out to study the hydraulic contribution and quantify the associated uncertainty. To achieve this objective, we develop a multi-stage approach to carry out an initial sensitivity analysis, highlighting the most influential parameters in the hydraulic model. By optimally adjusting these parameters, we aim to obtain a more accurate description of the flow redistribution phenomenon in the reactor core.The aim of the sensitivity analysis presented in this article is to construct an accurate and suitable surrogate model that represents the redistribution model in the core. This surrogate model will then be coupled with the thermomechanical model to quantify the final uncertainty in the simulation of fuel assembly deformation within a pressurised water reactor. This approach will provide a better understanding of the interactions between hydraulic and thermomechanical phenomena, thereby improving the reliability and accuracy of the simulation results.

1 INTRODUCTION

1.1 Industrial Issue

The rapid insertion of control rod clusters is of crucial importance for safety, as it allows for the quick reduction or immediate shutdown of the reactor power, ensuring control of reactivity, which is one of the fundamental safety functions during operation situations. Since the 1990s, several incidents of incomplete insertion of control rods have occurred, potentially jeopardizing this safety

function. The first event took place in 1994 in the Ringhals 4 reactor, when a control rod failed to fully insert after an emergency reactor shutdown, root cause investigation showed that the incomplete rod insertion (IRI) was caused by increased friction between the control rod and the assemblys guide thimbles [1]. In other words, the control rods slide within the guide tubes, and when the assembly is deformed, the guide tubes are deformed in the same manner, resulting in friction between the guide tubes and the control bars, preventing their complete insertion. In the following years, several other incidents of incomplete control rod insertion and increased control rod insertion times were detected in various Western reactors [2]. In German pressurized water reactors, increased permanent deformations of fuel assemblies have been observed since the year 2000 [3]. Both the extent of deformations and the frequency of occurrences had increased since then until the early 2010s, when several events related to fuel assemblies deformation were reported in different nuclear power plants. In a unique case, an incident of incomplete control rod insertion occurred. In several other cases, increased control rod insertion times were measured, exceeding the specified maximum values. In most of the mentioned cases, a collective deformation of fuel assembly across the entire core was observed. Individual fuel assembly can exhibit deformation amplitudes of up to 25 *mm* at maximum and are generally deformed into one of the three characteristic shapes, namely a *C*, *S*, or *W* shape (see Figure 1).

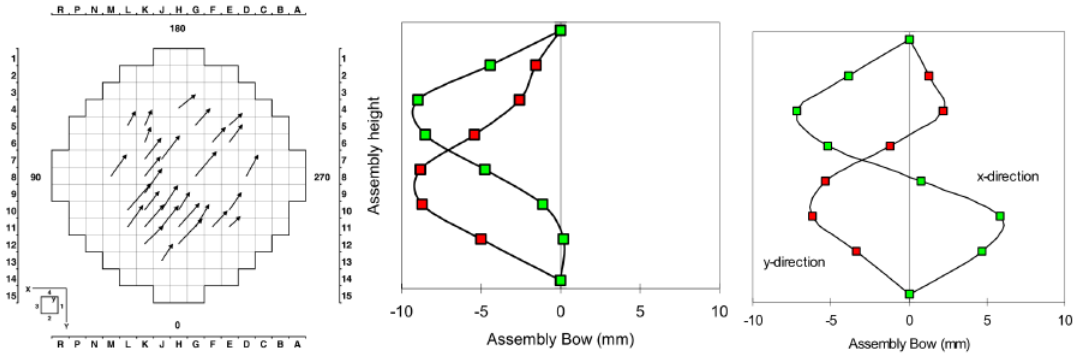

Figure 1: Collective deformation of fuel assemblies measured at Ringhals 2 (left), C-shaped deformations measured at Ringhals 3 (middle), and S-shaped deformations measured at Ringhals 4 (right) (From [1]).

1.2 Bow influencing mechanisms

Over the years, a multitude of mechanisms (see figure 2) have been discussed as the origins of fuel assembly bow or as factors that promote it. In general, two types of mechanisms influencing deformation must be distinguished: inducing mechanisms and reinforcing mechanisms. Inducing mechanisms are those that initiate deformation by creating bending moments within the structure. Reinforcing mechanisms are those that cannot cause deformation by themselves but significantly influence how it occurs and at what rate. The final deformation patterns are likely the result of the interaction between different mechanisms, making it difficult to determine and quantify the contribution of each individual effect. This coupling of multiple mechanisms, coupled with the mechanical coupling of fuel assemblies within the reactor core, can potentially lead to counter-intuitive and self-amplifying effects, possibly explaining the emergence of heavily deformed cores with asymmetric deformation patterns. The main mechanisms influencing the deformation of fuel

assemblies are mentioned in [4], [5], [6], and they can be summarized as follows: Hold down forces, structural growth, structural creep, fuel assembly stiffness, grid spring relaxation, lateral mechanical coupling, fast neutron irradiation, and lateral hydraulic forces.

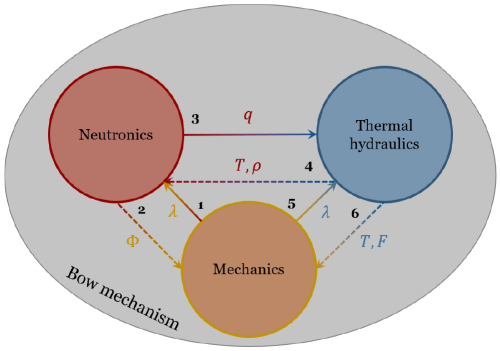

Figure 2: Physical interactions during the deformation of the assembly (From [7])

1.3 Literature review on uncertainty quantification in the context of fuel assembly deformation and motivation for our work

In exploring existing literature, we observed that the majority of studies focusing on uncertainty quantification are situated within a specific framework centered around phenomena contributing to fuel assembly deformation, or those influencing it, rather than the simulation of the deformation phenomenon itself. Many works address the uncertainty associated with neutron flux calculations, such as Laura Clouvel's thesis in 2019 [8]. Furthermore, sources of uncertainty related to grid-to-rod fretting, which is the subject of Pernice's research in 2012 [9], are also discussed, given that grid-to-rod fretting and penetration are the primary causes of fuel failure in pressurized water reactors. However, Wanninger conducted more extensive sensitivity and uncertainty analysis in 2018 [4] to assess the model's reactivity to various influencing mechanics. Sensitivity analysis work in the context of phenomena contributing to fuel assembly deformation, particularly concerning hydraulic calculations, was carried out by de Lambert [10].
According to what has been discussed in the literature, it is clearly evident that considering uncertainties during the numerical simulation of assembly deformations is of crucial importance. However, previous works have mainly sought to highlight this importance, but their results remain limited and highly focused on particular objectives. Our work aims to overcome these limitations by focusing on quantifying uncertainties that propagate through a nonlinear thermohydraulic and thermomechanical coupling. The central idea is to develop an efficient methodology capable of adapting to the multidimensional and multiphysics nature of this simulation, as well as the associated multifidelity approach. In other words, our main objective is to propose a methodological framework that addresses all these challenges.

1.4 Summary of the objectives of this article

In the context of this study, our focus is initially analyzing the hydraulic contribution to the deformation of fuel assemblies. This article aims to explore in detail the various aspects of this complex relationship. Specifically, our work is divided into several parts aiming to deepen our understand-

ing of these interactions. Section 2 is devoted to an initial investigation: evaluating the spatial propagation of local deformation in fuel assemblies due to hydraulic forces. This involves assessing the distance at which the thickness variation of a water gap ceases to have a significant influence on hydraulic forces. In continuation, we address in the same section a study on the linearity of the hydraulic model. This investigation aims to select a surrogate model that can adequately represent the hydraulic model. Section 3 marks a turning point towards the development of a methodology dedicated to the sensitivity analysis [11] of the hydraulic model. We intend to explore the range of deformations, ranging from small to large values, with the aim of creating a surrogate model, suitable for coupling with mechanics, using the Gaussian process technique presented in [12]. The focus will be on developing a robust approach to identify key parameters of the hydraulic model that most significantly influence fuel assembly deformations.
In summary, this article aims to provide a comprehensive overview of the relationship between assembly deformations and hydraulic forces. Through the analysis of deformation propagation, characterization of the linearity of the hydraulic model, and the development of a sensitivity analysis methodology, we seek to create relevant statistical tools for subsequent applications, particularly coupling with mechanics.

2 PRELIMINARY STUDY OF HYDRAULIC CONTRIBUTION

Hydraulic forces play a crucial role in the deformation of fuel assemblies, resulting from complex phenomena occurring within the reactor core. Among these phenomena, macroscopic flow redistribution are induced by differences in behavior between the inlet and outlet. Furthermore, local-scale redistribution are observed, such as significant redistribution upstream of the grids. The grids of the fuel assemblies exert a significant influence on the flow within the reactor. When the assembly undergoes deformation, the dimensions of the spaces between the grids are affected. This variation affects the flow distribution between the grids, leading to disparities in pressure applied to the opposite outer sides of the same grid. Consequently, a lateral hydraulic force forms, contributing to the lateral deformation of the assembly (see Figure 3).

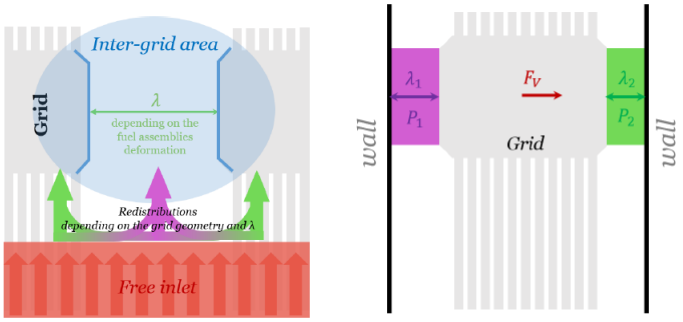

Figure 3: Flow redistribution in the core (left), lateral hydraulic force (right) (From [7])

The main objective is to characterize the flow existing between two adjacent grids by modeling it using the extended Bernoulli's equation. Considering a streamline [AB], the relation (without gravity) between the flow velocity and pressure is given by:

$$P_A + \frac{1}{2}\rho V_A^2 = P_B + \frac{1}{2}\rho V_B^2 + \Delta P \tag{1}$$

where P represents the pressure, V the bulk velocity, ΔP the irreversible pressure loss between A and B, $\Delta P = KQ^{\alpha}$ with the exponent α depending on the formula used, K the hydraulic resistance coefficient, and Q the volumetric flow rate of water. Consequently, in-core flow redistribution can be modeled with a pipe hydraulic network. All hydraulic simulations presented in this paper were calculated using a tool called Phorcys. The latter is used for evaluating the redistribution of volumetric flow rates in hydraulic networks (for more details, we refer to [7]).
For the hydraulic code Phorcys, a number of input data exhibit uncertainty, whether it is of epistemic nature (resulting from a lack of knowledge or information) or stochastic nature (stemming from natural fluctuations of certain phenomena). To grasp this uncertainty, a multi-step methodology has been developed to study the aforementioned code.
The objective of this initial study is to assess the spatial propagation in Phorcys results due to a local perturbation of input parameters. This involves determining the distance at which the variation in thickness of a water gap, represented by λ, ceases to have a significant influence on hydraulic forces. Secondly, the aim is to evaluate the level of non-linearity between this local perturbation (λ) and its effect (force). These objectives are geared towards establishing an appropriate method for conducting an initial sensitivity analysis.

2.1 Dimension reduction applied to the description of the deformed core

The methodology adopted in this study involves considering 15 assemblies aligned in the plane of the Phorcys code and perturbing a specific assembly. The objective is to measure the decrease in perturbed hydraulic forces as a function of distance (assembly position). To simplify the complexity, a dimensional reduction is performed by representing the displacements of the 10 grids within an assembly using only 3 carefully chosen modes, denoted as C, S, W [13] (see Figure 4). Subsequently, the fields of hydraulic forces resulting from the deformed mode are compared to those of the undeformed mode (straight assembly) $\Delta F_h = F_h(deformed) - F_h(straight)$. This comparison will assess the impact of the various deformation modes on hydraulic forces.

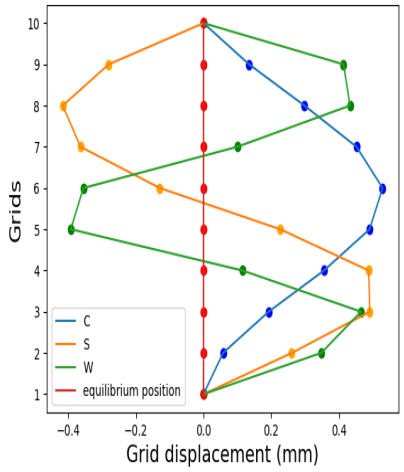

Figure 4: Representation of the 3 deformation modes C, S, W

2.2 Choice of boundary conditions

In this study, four different velocity profiles for the flow at the lower plate of the core (bottom of the assemblies) are considered: Horvath [14], parabolic, homogeneous, and offset (see Figure 5). The average velocity at the inlet of the assembly is fixed at 5 m/s. The results obtained are presented in the form of perturbations, where ΔF_h represents the difference between the hydraulic forces F_h observed with deformed assemblies (deformed AC) and straight assemblies (straight AC). This approach allows us to assess the influence of different velocity and deformation conditions on hydraulic forces.

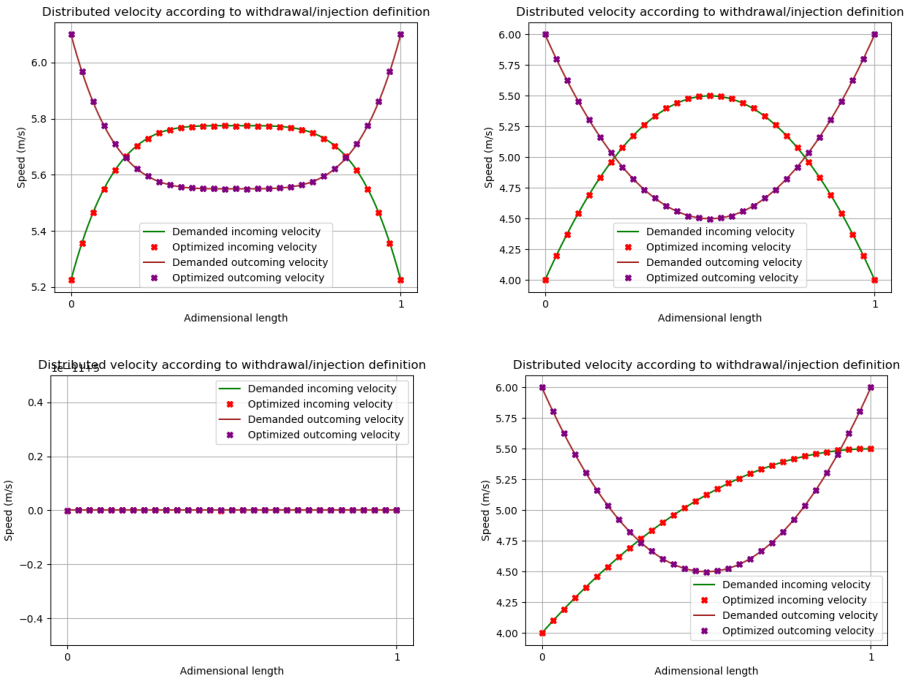

Figure 5: Profiles: Horvath (top left), parabolic (top right), homogeneous (bottom left), and offset (bottom right). We note that the requested profile is the one specified by the user, while the optimized profile is calculated by Phorcys for mass conservation.

2.3 The impact of a fuel assembly deformation on hydraulic forces

In this section, we present the results of lateral hydraulic force variation due to the deformation of a single fuel assembly located in the middle of row A_8 and two neighboring assemblies A_8 and A_9 simultaneously, also positioned in the middle. Calculations were performed using different velocity profiles for all three deformation modes and also on the peripheral assemblies located near the periphery (A_2, A_3) and (A_{13}, A_{14}) close to the reactor vessel. However, we only present the results obtained with the Horvath profile [14], which is an illustrative case, and the deformation mode C (see Figure 6).

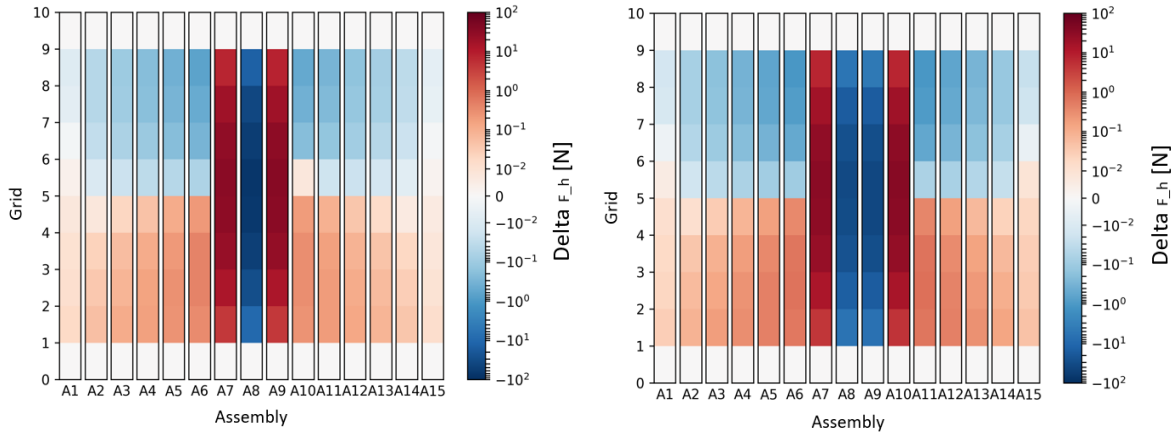

Figure 6: Spatial distribution of ΔF_h after A_8 deformation (left figure), and for A_8 and A_9 (right figure) simultaneously

The presented results clearly show that the deformation of an assembly only affects the hydraulic forces on the assembly itself as well as on its nearest neighbors. This observation holds true for all velocity profiles mentioned earlier and also for all deformation modes in the case of small deformations, i.e. where the maximum amplitude of the mode is less than or equal to 2 mm, which is the nominal value of the water gap (distance between 2 grids).

2.4 Study of the linearity of the hydraulic model

In order to choose the most appropriate method to construct a surrogate model adapted to the hydraulic aspect, it is interesting to study the behavior of hydraulic forces in relation to the deformations of fuel assemblies. To achieve this, several studies have been conducted, and we detail them in this section.

Case of small deformations In this paragraph, we address the case of small deformations, which represent a realistic scenario for new assemblies that are still slightly deformed. Small deformations are characterized by water gap thicknesses close to 2 *mm* and the absence of contact between the assemblies. Three studies were conducted to test the linearity of hydraulic forces output: The first study is to test local linearity on an assembly, to verify if $\Delta F_h(K.\mathrm{Mod}_i(A_8)) = K.\Delta F_h(\mathrm{Mod}_i(A_8))$, the second one is to test the linearity of the linear combination of $(C+S+W)$ and $(C+S-W)$ on an assembly $(\Delta F_h(K.\Sigma\mathrm{Mod}_i(A_8)) = K.\Sigma(\Delta F_h(\mathrm{Mod}_i(A_8)))$, and the third study is to test a simultaneous perturbation of (A_8 and A_9) $(\Delta F_h(K.\Sigma\mathrm{Mod}_i(A_8+A_9)) = K.\Sigma(\Delta F_h(\mathrm{Mod}_i(A_8+A_9)))$. All cases have been tested, and we will present the case of the linear combination of the 3 deformation modes on a single assembly, namely $(C+S+W)$ (Figure 7), since the results of all our tests were similar.
According to the results in Figure 8, one can observe the linearity of hydraulic forces concerning the amplitude of deformation in the case of small deformations. It is noteworthy that this linearity is generally preserved even in the case of a heterogeneous and off-centered flow that was tested. These findings are important as they provide valuable information to guide metamodelling and facilitate the understanding of hydraulic forces in real conditions where the flow can be heterogeneous and off-centered.

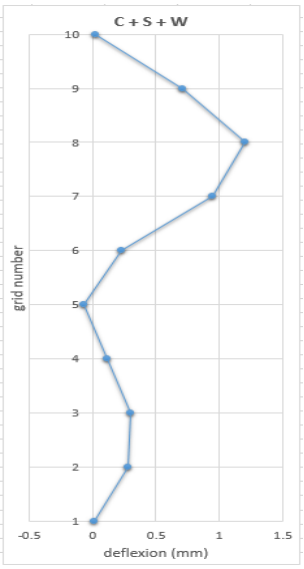

Figure 7: Mode (C+S+W)

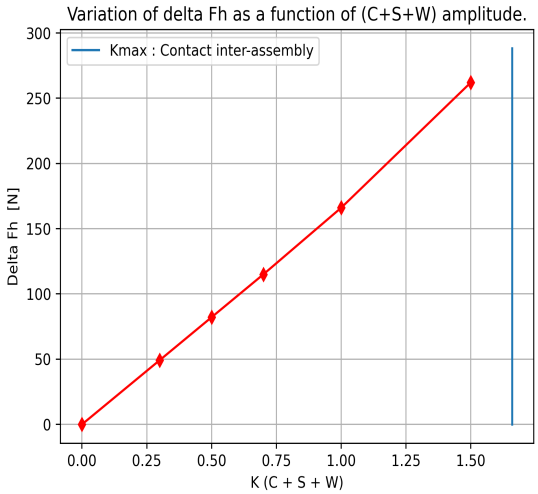

Figure 8: Variation of ΔF_h as function of (C+S+W) amplitude

Case of large central water gaps Now, we focus on the case of a strongly deformed barrel-shaped core, meaning with a water gap of about 10 to 20 *mm* at the center of the core, and consequently, a majority of assemblies deformed on either side (see Figure 9). This geometric configuration is commonly observed at the end of power cycles (which last approximately one year). To do this, we will consider different values of central water gaps, namely 5, 10, 15, and 20 *mm*, and analyze the corresponding response of hydraulic forces.

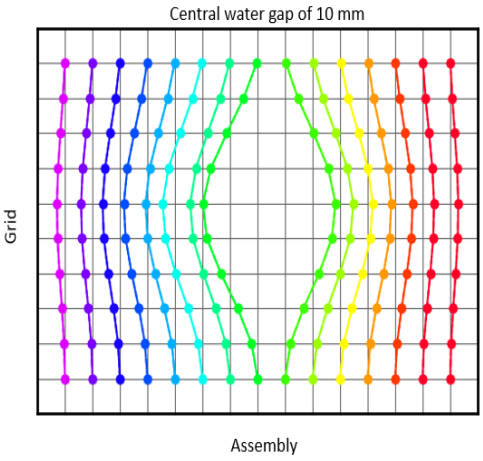

Figure 9: Central water gap of 10 *mm*

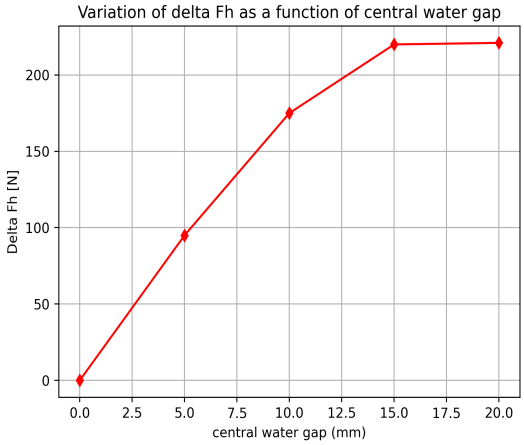

Figure 10: Variation of ΔF_h as function of central water gap

We clearly observe a loss of linearity when the large water gap exceeds 10 *mm* (see Figure 10). The results obtained confirm that hydraulic forces do not follow a linear relationship beyond a certain critical value of the water gap. This loss of linearity is consistent with findings from DIVA+G experiments in [15, Figure 15]. These observations highlight the importance of considering this non-linearity in hydraulic models. When water gaps exceed the critical threshold, it becomes necessary to use nonlinear approaches to accurately describe the behavior of hydraulic forces.

These findings contribute to improving our understanding of the interactions between water gaps and hydraulic forces, providing valuable insights for the development of more precise surrogate model tailored to real conditions.

Conclusion To conclude, concerning hydraulic forces contributing to the deformation of fuel assemblies, two distinct regimes can be identified based on the deformation level. In the regime of small deformations, hydraulic forces vary proportionally to deformations, and disturbances remain local. However, when examining the regime of large deformations, non-linearity is observed for water gaps exceeding 10 *mm*. To deepen our understanding of these phenomena, two orientations of sensitivity analysis have been considered. The first sensitivity analysis focuses on small deformations to assess their impact on hydraulic forces in the quasi-linear regime. The second sensitivity analysis, on the other hand, considers the case of large central water gaps where non-linearity is observed. These two orientations of sensitivity analysis will provide us with more detailed information about the behavior of hydraulic forces in different deformation regimes and quantify the uncertainty of the Phorcys code results.

3 SENSITIVITY ANALYSIS FOR HYDRAULIC MODEL

In this section, we perform a sensitivity analysis using the Sobol method [16] for both deformation regimes, namely, small and large deformations of fuel assemblies. The goal is to investigate how the uncertainty in the model output can be distributed among the various sources of uncertainty in the input parameters of the model [11]. We recall the definitions of the first-order and total Sobol indices. If $\mathbf{X} = (X^{(i)})_{i=1}^{d}$ is the vector of independent input parameters and Y is the scalar output, then

$$S_i = \frac{\mathrm{Var}(\mathbb{E}[Y|X^{(i)}])}{V}, \qquad T_i = \sum_{v \in \mathscr{P}, i \in v} S_v = 1 - \frac{\mathrm{Var}(\mathbb{E}[Y|\mathbf{X}^{(-i)}])}{V}, \tag{2}$$

where $V = \mathrm{Var}(Y)$, $\mathscr{P}$ is the set of subindices in $\{1,\dots,d\}$, $\mathbf{X}^{(-i)} = (X^{(1)},\dots,X^{(i-1)},X^{(i+1)},\dots,X^{(p)})$, and S_v is the high-order Sobol index $S_v = \mathrm{Var}(\mathbb{E}[Y|\mathbf{X}^{(v)}])/V$ with $\mathbf{X}^{(v)} = (X^{(i)})_{i \in v}$. S_i is the first-order index that measures the contribution to the output variance of the main effect of the ith input alone. T_i is the total index that measures the contribution to the output variance of the ith input, including all variance caused by its interactions with any other input variables.

3.1 A first sensitivity analysis: Case of small deformations

Motivated by the previous results, an initial sensitivity analysis is conducted to assess the impact of small deformations in the hydraulic model, which provides the forces to be applied in the thermo-mechanical calculation. To conduct this analysis, it is essential to consider all uncertain parameters of the code and assign them an appropriate probability distribution based on reliable bibliographic references. The goal of this initial sensitivity analysis is to understand how small deformations, along with other parameters, influence the results of the hydraulic model. The calculations of Sobol indices are performed using the Uranie platform of CEA: an open-source software for optimisation, meta-modelling and uncertainty analysis [17].

3.1.1 Uncertain parameters of the hydraulic model

Table 1 provides us with a definition of these parameters as well as the chosen probability distribution for each parameter, based on information from the cited references. V, M_{in}, L^{in}_{offset}, M_{out}, and L^{out}_{offset} are parameters that determine the boundary conditions at the inlet and outlet of the core.

Parameter	Definition	Distribution
C_{ij}	Modal coefficients	$\mathcal{N}\left(\mathbf{0}, \sigma_i^2 \mathbf{M}\right)$ [3.1.1]
$T\ (^\circ C)$	Temperature	$\mathcal{N}(\mu = 300, \sigma^2 = 11.08)$ [18]
$h_l\ (mm)$	Redistributing flow height	$\mathcal{U}(10, 30)$ [10]
C_g	Axial loss coefficient for a grid	$\mathcal{U}(1, 1.22)$ [19]
$V\ (m/s)$	Flow velocity	$\mathcal{N}(\mu = 5, \sigma^2 = 0.05^2)$ [20]
M_{in}	flattening of the parabolic incoming velocity profile	$\mathcal{N}(\mu = 0.05, \sigma^2 = 0.005^2)$ [20]
L^{in}_{offset}	Offsetting of the parabolic incoming velocity profile	$\mathcal{N}(\mu = 0, \sigma^2 = 0.2^2)$ [21]
M_{out}	flattening of the parabolic outgoing velocity profile	$\mathcal{N}(\mu = 0.04, \sigma^2 = 0.004^2)$ [20]
L^{out}_{offset}	Offsetting of the parabolic outgoing velocity profile	$\mathcal{N}(\mu = 0, \sigma^2 = 0.1^2)$ [21]

Table 1: Table of uncertain input parameters and their probability distributions

h_l parameter: The model 3 presented in [10], which includes a resistance to flow leakage, requires defining the parameter h_l, corresponding to the height used to calculate the lateral pressure drop ΔP_l. The example shown in [10, Figure 12] demonstrates that the flow redistribution (from the bypass to the grids) starts at a distance h_l upstream of the grid. It has also been observed that when the value of h_l exceeds 30 mm, it does not affect the flow or the pressure drop, as a quasi-asymptotic regime is reached beyond this value (see [10, Figure 26]). However, there is a singular point when λ and h_l approach 0, where the upstream pressure drop associated with flow redistribution becomes potentially infinite. This is logical since this singular point corresponds to a situation in which almost all incoming flow would be forced to pass through the grids ($\lambda = 0$) through an extremely narrow horizontal gap ($h_l = 0$). Therefore, it is important not to choose a value that is too small for this parameter. In conclusion, we opted for a uniform distribution for h_l, $h_l \sim \mathcal{U}(10, 30)$.
C_{ij} the modal coefficients: We chose to create an orthonormal family of 3 deformation modes, denoted as C, S, and W (see Figure 4) to represent the deformation of each assembly by projecting the displacements onto these three modes. This enables us to represent the deformation of an assembly with only 3 amplitudes in the *xoz* plane and 3 other amplitudes in the *yoz* plane for a 3D calculation. This already leads to a significant dimensional reduction in describing the assemblies' deformations. Moreover, the water gaps (defined in section 2) can also be expressed in this same family as they are algebraically derived from the assemblies' deformation. Initially, we aim to conduct an initial sensitivity analysis using a row of 15 assemblies. As already demonstrated, the water gaps λ are expressed in terms of the modes C, S, and W as follows: $\lambda_j(z) = \sum_{i=1}^{3} C_{ij} f_i(z) + \lambda_0$, where i is the mode index, $j = 1, ..., n_\lambda = 16$ is the index of the water gap, C_{ij} represents the modal coefficient, $f_i(z)$ corresponds to the lateral displacement mode of the assembly expressed in terms of heights z of all grids: $z = 1, ..., 10$. $\lambda_0 = 2$ mm is the nominal value of λ (in the case of undistorted assemblies). As the core is constructed in an axisymmetric manner, the C_{ij} can be positive or negative depending on the direction of movement. We choose each C_{ij} to follow a normal distribution with zero mean and standard deviation σ ($C_{ij} \sim \mathcal{N}(\mu = 0, \sigma)$). First, there are two physical conditions to verify: the **inter-assembly non-penetration constraint** and the **conservation of the**

total distance. In the case of small disturbances in the water gaps, the first constraint will be automatically satisfied. As for the second constraint, considering that the assemblies are placed inside the vessel, which has a constant diameter, and are uniformly distributed over the total distance of the vessel with a nominal gap of $\lambda_0 = 2$ *mm* between assemblies and between peripheral assemblies and the vessel, for undeformed assemblies, this implies that for a row of 15 assemblies, the total clearance is equal to $n_\lambda . \lambda_0 = 32$ *mm*. These constraints can be expressed after projection onto the family of the three modes as follows. The first constraint is $\sum_{i=1}^{3} C_{ij} f_i(z) + \lambda_0 \geq 0 \ \forall j, z$, and the second one is $\sum_{j=1}^{n_\lambda} \sum_{i=1}^{3} (C_{ij} f_i(z) + \lambda_0) = n_\lambda \lambda_0 \ \forall z$. It is deduced that to verify the constraint of total distance conservation, it is necessary to condition by $\sum_{j=1}^{n_\lambda} C_{ij} = 0$ for all i. To do this, we use Theorem of Gaussian conditioning. Denoting $Y_1 = (C_i)_{i=1}^{n_\lambda}$ and $Y_2 = \sum_{j=1}^{n_\lambda} C_j$, the distribution of Y_1 given $Y_2 = y_2$ is

$$\mathscr{L}(Y_1 \mid Y_2 = y_2) = \mathscr{N}\left(\mathbf{R}_{12} R_{22}^{-1} y_2, \mathbf{R}_{11} - \mathbf{R}_{12} R_{22}^{-1} \mathbf{R}_{21}\right),$$

with $\mathbf{R}_{11} = \sigma^2 \mathbf{I}$ where $\mathbf{I}$ the $n_\lambda \times n_\lambda$ identity matix, $\mathbf{R}_{12} = \sigma^2 (1, \ldots, 1)^T$, $\mathbf{R}_{21} = \mathbf{R}_{12}^T$, $R_{22} = n_\lambda \sigma^2$. With $y_2 = 0$, we can conclude that :

$$\mathscr{L}(Y_1 \mid Y_2 = 0) = \mathscr{N}\left(\mu', \Sigma'\right) \text{ with } \mu' = (0, \ldots, 0)^T \text{of size } n_\lambda, \Sigma' = \sigma^2 \mathbf{M}$$

with $\mathbf{M} = \mathbf{I} - n_\lambda^{-1} \mathbf{U}$ and $\mathbf{U}$ the $n_\lambda \times n_\lambda$ matrix full of ones. It is noted that the variance of the coefficients C_i after conditioning is $\sigma^2(1 - 1/n_\lambda)$. If this is the value to be imposed, then σ^2 should be taken equal to this value divided by $1 - 1/n_\lambda$.
We also know that modes S and especially W always have amplitudes lower than that of mode C. Therefore, it suffices to choose a standard deviation σ_c for $C_j(c)$ larger than σ_s and σ_w for $C_j(s)$ and $C_j(w)$. This strategy allows us to conduct an initial sensitivity analysis with the 3 independent vectors:

- $C = C_{1j} \sim \mathscr{N}(\mu_c, \Sigma_c)$ avec : $\mu_c = (0, ..., 0)^T$ of size $n = 16, \Sigma_c = \sigma_c^2 \mathbf{M}$.
- $S = C_{2j} \sim \mathscr{N}(\mu_s, \Sigma_s)$ avec : $\mu_s = (0, ..., 0)^T$ of size $n = 16, \Sigma_s = \sigma_s^2 \mathbf{M}$.
- $W = C_{3j} \sim \mathscr{N}(\mu_w, \Sigma_w)$ avec : $\mu_w = (0, ..., 0)^T$ of size $n = 16, \Sigma_w = \sigma_w^2 \mathbf{M}$.

3.1.2 A Sobol sensitivity analysis on the force at each grid level

To give a physical meaning to our study, we decided to perform a Sobol sensitivity analysis for each grid in the row of 15 assemblies. We choose the lateral hydraulic force exerted on each grid as the quantity of interest to observe the spatial variation of dependencies. We only present the results for grids 2 to 9, as grids 1 and 10 are fixed. We find that the Sobol indices for hydraulic forces at each grid level for both first-order and total effects are almost equal. This allows us to conclude that there is small interaction between the parameters. Therefore, we present the results of the first-order Sobol indices at each grid level. The results are presented in the form of circular diagrams (see Figure 11) to provide an idea of the most influential parameters at each grid level for each assembly.
Analysis of the results: In this analysis on the hydraulic forces at different grid levels (from height 2 to height 9), the results indicate that the most influential parameters vary with height. At

grid levels 2 to 4, hydraulic forces are primarily influenced by the offset of the velocity profile parabola ($l_{off_{in}}$) and the epistemic parameter h_l, as deformations are negligible in these regions. As the observation moves up to grids 5 to 8, the deformation mode C becomes the most influential parameter, closely followed by h_l. Mode C exhibits higher amplitudes and clearly dominates at grid level 6. Deformation modes S and W also influence areas where their amplitudes are maximal. Finally, at grid level 9 near the upper plenum, the epistemic parameter h_l along with velocity profile parameters become dominant.

After calculating the Sobol indices, we also present the spatial distribution of standard deviations across a series of 15 assemblies (see Figure 12) to identify locations where they are high. According to the obtained results, it is evident that the greatest dispersion is observed at grid levels 5 and 6, where the amplitude of mode C is maximal. These findings align with those obtained during the Sobol analysis.

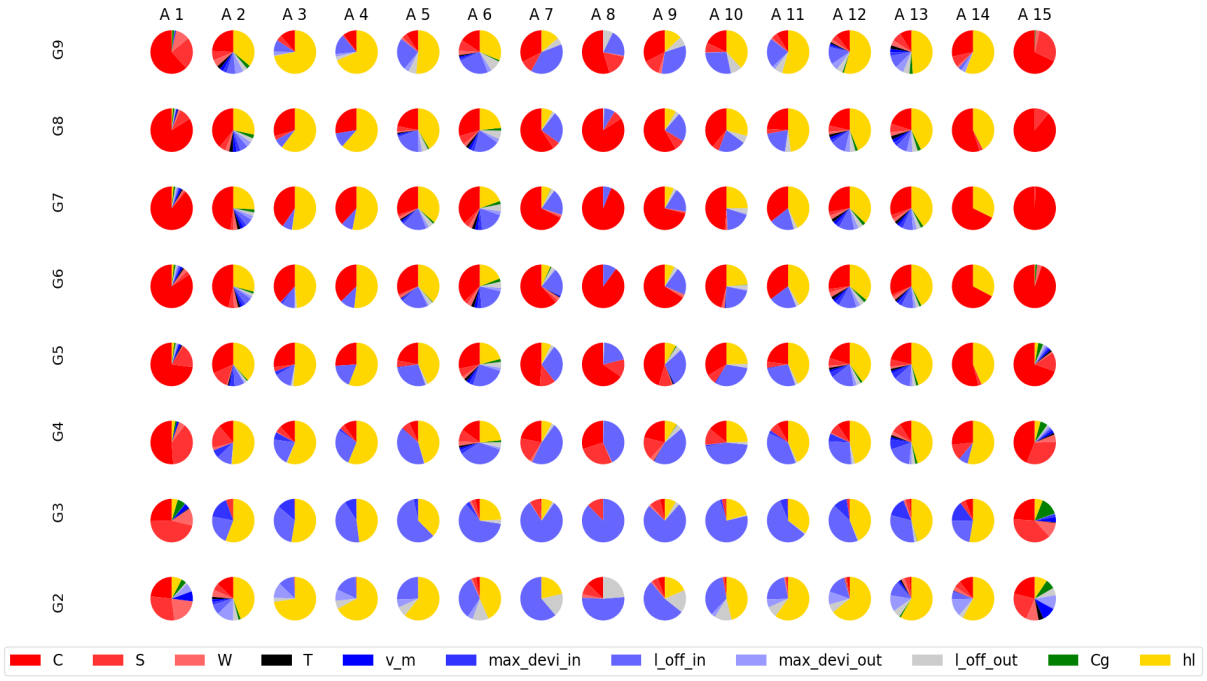

Figure 11: Spatial distribution of first-order Sobol indices for evaluating lateral force at each grid level.

Conclusion : This study enabled us to examine the spatial distribution of the Sobol indices in great detail. This enabled us to observe, in a very local and precise way, what is happening at the level of each grid of the 15 assemblages, and to classify the most influential parameters for each grid of each assembly. In addition, we were able to adopt a more global perspective by examining all the grids at the same height, which enabled us to analyse the results at the entry, within and exit of the core, and to identify the most influential parameters on the hydraulic forces. In summary, we found the significant effect of the boundary conditions at the core inlet and outlet, which, in the absence of any deformation of the assemblies, are the main cause of the velocity gradients, which in turn create the hydraulic forces. It is worth highlighting the remarkable influence of the epistemic parameter h_l, which always remains influential and comparable to that of small deformations.

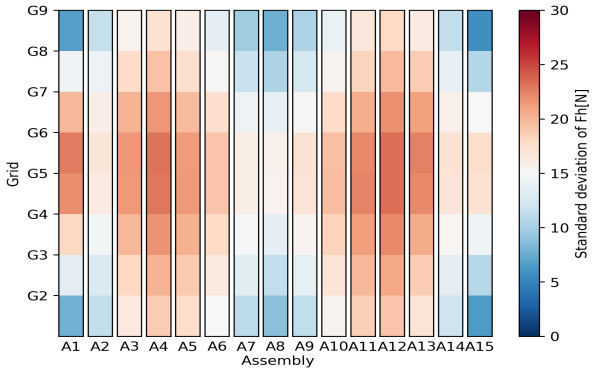

Figure 12: Spatial distribution of the standard deviation of F_h

3.2 A second sensitivity analysis: Case of large deformations

In this section, we focus on the sensitivity analysis of the hydraulic model in the context of large deformations. To achieve this, we apply a deformation of 20 *mm* (see Figure 13) between A_8 and A_9, with the aim of identifying the epistemic and stochastic parameters that exert the greatest influence on the hydraulic forces. Since the deformation has been fixed, this results in the absence of modal coefficients C_{ij}.

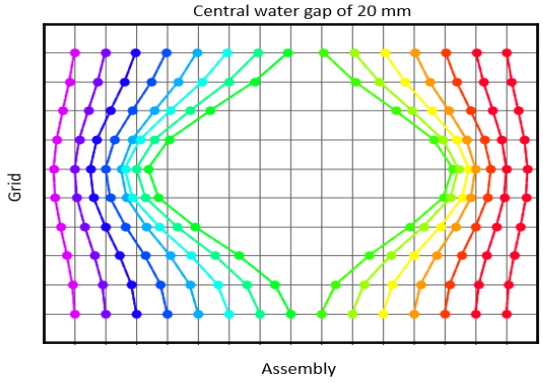

Figure 13: 20 *mm* water gap imposed for the sensitivity analysis

According to the results shown in Figure 14, it is evident that on grids 2 and 3, where the deformation amplitude is generally moderate, the influence of boundary conditions is very clear in addition to the parameter h_l. These findings are consistent and compatible with our previous analysis because in the absence of any assembly deformation, only velocity gradients created by non-uniform profiles can generate hydraulic forces. Furthermore, it is clearly demonstrated that the epistemic parameter h_l dominates in areas of significant deformations and in transverse flow areas, where the assemblies are in contact, or nearly in contact. In conclusion, in the regime of large deformations, the epistemic parameter h_l remains the most influential, followed by the parameter $l_{off_{in}}$, which represents one of the boundary condition parameters.

We then decided to present the spatial distribution of standard deviations over a series of 15 assemblies (see Figure 15) to identify the locations where these deviations are the highest. It is clearly observable that the maximum standard deviation values are located in the middle zone of the 15 assemblies, where we applied our large deformation. This analysis shows that the variance of

hydraulic forces increases in the case of a very significant water gap.

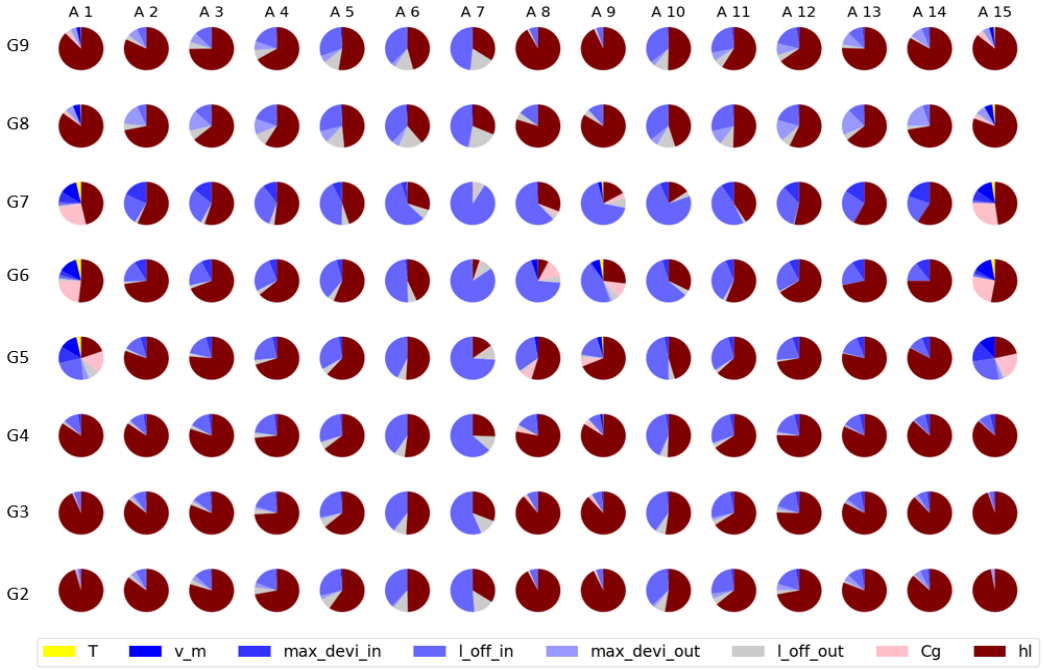

Figure 14: Spatial distribution of first-order Sobol indices for evaluating lateral force at each grid level.

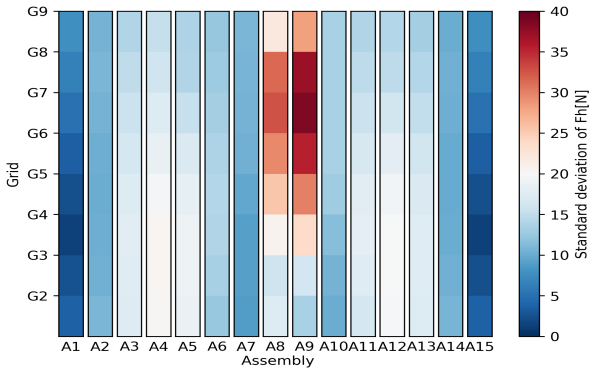

Figure 15: Spatial distribution of the standard deviation of F_h

4 SURROGATE MODELING OF HYDRAULIC MODEL USING GAUSSIAN PROCESS

In the context of our study on hydraulic forces, it is essential to select an appropriate surrogate model to represent them, which will be used later as input data for mechanics and is crucial for coupling. An accurate metamodel is also necessary to carry out uncertainty quantification and quantitative sensitivity analysis (such as Sobol' method [16]). Motivated by the need to quantify the uncertainties, we have chosen to build Gaussian process metamodels. Since the hydraulic model shows no irregularities, we have chosen to use the tensorized Matérn covariance kernel

with the parameter $\nu = 3/2$. Considering the quasi-linear nature of the hydraulic forces model under investigation, we decided to adopt a linear trend for the Gaussian process. The outputs of interest in our study are the hydraulic forces at each grid level. To assess the performance of our model, we calculate a Gaussian process for each scalar output. This measure provides valuable insights into the quality of the model predictions for the force at each grid level. Regarding the estimation of the model's hyperparameters (variance and scalelengths), we opted for the Leave-One-Out (LOO) method [17]. In figure 16 left we present the spatial distribution of the factor Q^2, also known as the predictivity coefficient. It is estimated using a test dataset, denoted as $\mathscr{P} = \{(x^{(j)}, y^{(j)}) : j = 1, ..., n_s\}$, comprising another set of realizations. Its size is denoted as n_p. It is calculated using the formula:

$$Q^2 = 1 - \frac{\sum_{j=1}^{n_p} \left(y^{(j)} - \hat{y}\left(\mathbf{x}^{(j)}\right)\right)^2}{\sum_{j=1}^{n_p} \left(y^{(j)} - \bar{y}_{test}\right)^2}, \quad \mathbf{x}^{(j)} \in \mathscr{P} \tag{3}$$

where $\bar{y}_{test}$ is the mean of the quantity of interest in the test basis, $y^{(j)}$ is the observed value, and $\hat{y}(\mathbf{x}^{(j)})$ is the predicted value. We also present the standard deviations of the prediction of the Gaussian process at each grid level in figure 16 right. We notice that the quality factors for the Gaussian processes at all grid levels are greater than 0.8. Moreover, the overall average value of $Q^2 = 0.93$ confirms the predictive efficiency of the Gaussian process, thus validating its large-scale use. Predictive standard deviations are larger in areas where the prediction has a lower Q^2, which shows that the predictive uncertainty is well quantified.

In conclusion, surrogate modeling by Gaussian process regression has proven effective in predicting hydraulic force at each grid level. We successfully represented hydraulic forces on each grid using a Gaussian process, establishing a reliable and accurate surrogate model within the regime of small deformations. This surrogate must cover both the deformations for coupling and the epistemic parameters for the propagation of uncertainty.

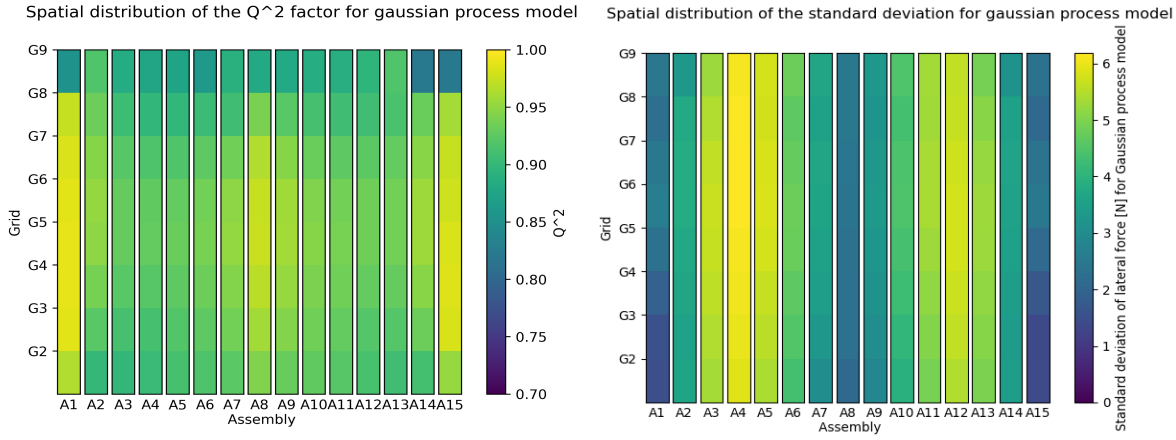

Figure 16: Left: Spatial distribution of the Q^2 factor for Gaussian process model. Right: Spatial distribution of the standard deviation of prediction for the Gaussian process model

5 CONCLUSION

This article presents a comprehensive analysis of uncertainty in the simulation of lateral hydraulic forces, focusing on the hydraulic code PHORCYS. Section 2 identifies two behavior regimes: linear for small deformations and nonlinear beyond 10 *mm* of water gap thickness. A Sobol sensitivity analysis in Section 3 reveals the predominant influence of deformation mode C and the epistemic parameter h_l, as well as the significant impact of boundary conditions. The spatial study of Sobol indices at the level of force on each grid confirms these findings, emphasizing the importance of h_l and boundary conditions. In Section 4, an efficient hydraulic metamodel is created for hydraulic forces in the regime of small deformations, which will be valuable for exploring this simulation's contribution to the overall uncertainty of the problem when coupled with mechanics in future work.

Acknowledgements We thank Nicolas Lamorte (Framatome) for stimulating and useful discussions.

References

[1] T. Andersson, J. Almberger, and L. Björnkvist. "A Decade of Assembly Bow Management at Ringhals". In *IAEA-TECDOC-1454 Structural Behaviour of Fuel Assemblies for Water Cooled Reactors*, pages 129–136, Vienna, Austria, July 2005. IAEA.

[2] S. Roudier and R. Béraha. "Nuclear Fuel in France: an ever changing world - most recent safety concerns of DSIN". In *Specialist Meeting on Nuclear Fuel and Control Rods: Operating Experience, Design Evolution and Safety Aspects*, pages 63–77, Madrid, Spain, November 5-7 1996. OECD-NEA.

[3] RSK. "Verformungen von Brennelementen in deutschen Druckwasserreaktoren (DWR). RSK-Stellungnahme". 474. Sitzung der Reaktor-Sicherheitskommission (RSK) am 18.03.2015, 2015.

[4] A. Wanninger, M. Seidl, and R. Macián-Juan. "Mechanical analysis of the bow deformation of a row of fuel assemblies in a PWR core". *Nuclear Engineering and Technology*, 50:297–305, 2018.

[5] N. Lamorte, E. Méry de Montigny, N. Goreaud, B. Chazot, and V. Marx. "Advanced Predictive Tool for Fuel Assembly Bow Design Performance Evaluations". *Proceedings of the TOP FUEL Conference*, September 24-28 2021.

[6] C. Lascar, J. Champigny, A. Chatelain, B. Chazot, N. Goreaud, E. Mery de Montigny, J. Pacull, and H. Salaün. "Advanced predictive tool for fuel assembly bow based on a 3D coupled FSI approach". *Proceedings of the TOP FUEL Conference*, September 13-17 2015.

[7] S. De Lambert. *"Contribution to the multiphysical analysis of fuel assembly bow"*. PhD thesis, 2021. 2021UPAST035.

[8] L. Clouvel. *"Uncertainty quantification of the fast flux calculation for a PWR vessel"*. Theses, Université Paris Saclay (COmUE), November 2019.

[9] M. Pernice. "Considerations for sensitivity analysis, uncertainty quantification, and data assimilation for grid-to-rod fretting". 10 2012.

[10] S. de Lambert, J. Cardolaccia, V. Faucher, O. Thomine, B. Leturcq, and G. Campioni. "Semi-analytical modeling of the flow redistribution upstream from the mixing grids in a context of nuclear fuel assembly bow". *Nuclear Engineering and Design*, 371:110940, 2021.

[11] A. Saltelli, S. Tarantola, F. Campolongo, and M. Ratto. *"Sensitivity Analysis in Practice: A Guide to Assessing Scientific Models"*. 2004.

[12] C. E. Rasmussen and Christopher K. I. Williams. *"Gaussian Processes for Machine Learning"*, volume 2. MIT Press, Cambridge, MA, 2006.

[13] A. Franzen. "Evaluation of Fuel Assembly Bow Penalty Peaking Factors for Ringhals 3 : Based on a Cycle Specific Core Water Gap Distribution". *Uppsala University, Applied Nuclear Physics*, 2017.

[14] A. Horváth and B. Dressel. "On numerical simulation of fuel assembly bow in pressurized water reactors". *Nuclear Engineering and Design*, 265:814–825, 2013.

[15] J. Cardolaccia and S. de Lambert. "Investigation of the flow redistribution upstream of grid-like obstacles separated by a variable gap". *Experimental Thermal and Fluid Science*, 121:110289, 2021.

[16] I. M. Sobol. Global sensitivity indices for nonlinear mathematical models and their monte carlo estimates. *Mathematics and computers in simulation*, 55(1-3):271–280, 2001.

[17] J.-B. Blanchard, G. Damblin, J.-M. Martinez, G. Arnaud, and F. Gaudier. "The Uranie platform: an open-source software for optimisation, meta-modelling and uncertainty analysis". *EPJ N - Nuclear Sciences & Technologies*, 5:4, January 2019.

[18] Jaerim Jang, Chidong Kong, Bamidele Ebiwonjumi, Alexey Cherezov, Yunki Jo, and Deokjung Lee. "Uncertainty quantification in decay heat calculation of spent nuclear fuel by STREAM/RAST-K". *Nuclear Engineering and Technology*, 53(9):2803–2815, 2021.

[19] Wang Kee In, Dong Seok Oh, and Tae Hyun Chun. "Empirical and Computational Pressure Drop Correlations for Pressurized Water Reactor Fuel Spacer Grids". *Nuclear Technology*, 139(1):72–79, 2002.

[20] J. Cardolaccia and S. de Lambert. "Investigation of the flow redistribution upstream of grid-like obstacles separated by a variable gap". *Experimental Thermal and Fluid Science*, 121:110289, 2021.

[21] A. Wanninger, M. Seidl, and R. Macián-Juan. "Mechanical analysis of the bow deformation of a row of fuel assemblies in a PWR core". *Nuclear Engineering and Technology*, 50(2):297–305, 2018. Special issue on the water reactor fuel performance meeting 2017 (WRFPM 2017).